Essential-Coupling-Path Models for Non-Contact EMI in Switching Power Converters Using Lumped Circuit Elements

N. K. Poon, *Member, IEEE*, Bryan M. H. Pong, *Senior Member, IEEE*, C. P. Liu, *Member, IEEE*, and Chi K. Tse, *Senior Member, IEEE*

***Abstract*—This paper proposes a simple lumped circuit modeling approach for describing noncontact EMI coupling mechanisms in switching power converters. The resulting model assumes a minimum number of noise sources and contains essential coupling paths that allow easy physical interpretations. Essentially, all capacitive couplings are represented by an equivalent noise voltage source and six coupling impedances, whereas all inductive couplings are represented by an equivalent noise current source and three coupling impedances. The resulting coupled noise appears as currents flowing into the terminals of the Line-Impedance-Stabilization-Network (LISN). The equivalent voltage source can be conveniently approximated as the switching-node-to-zero voltage, which is typically a rectangular pulse of a few hundred volts. The equivalent current source can be modeled as the current flowing around a loop containing the equivalent voltage source and parasitics such as winding capacitance of the power transformer, the snubber capacitance and connection inductances. Also, the coupling impedances can be estimated by making simplifying assumptions about the geometry of the components and tracks, or by direct measurements. Simulations and experiments verify how inductive and capacitive couplings through each path may produce substantial EMI measured by the LISN. Being based on a lumped circuit approach, the proposed model is easy to apply in practice for understanding, diagnosing and approximating EMI behaviors.**

***Index Terms*—Capacitive coupling, electromagnetic interference, inductive coupling, lumped circuit models, modeling.**

I. Introduction

ELECTROMAGNETIC INTERFERENCE (EMI) problems are usually complicated by the presence of coupling paths which do not show up explicitly in the formal circuit design. As a consequence, the formulation of effective solution approaches often relies on the engineer's experience or extensive numerical simulations based on some empirical models [1]–[4]. It will be desirable, from the engineer's point of view, if all noncontact EMI can be modeled by conventional lumped circuits which can be combined with the converter's circuit diagram to provide a full picture of the EMI conduction and coupling paths. Analysis and prediction can then be carried out with ease.

Lumped circuit models are proven to be adequate for analysis and prediction of EMI behaviors up to around 30 MHz [5]–[19]. In much of the prior works, knowledge of the significant paths is often crucial in the derivation of so-called simplified models for analysis. However, such knowledge can be hard to obtain in certain situations where the coupling paths could exist in a subtle manner. In this paper we propose a general lumped circuit model for analysis of all noncontact paths that give rise to EMI. Derived from a circuit theoretic viewpoint, this model contains all *essential coupling paths* that should be taken into consideration when evaluating the level of EMI that can be picked up by the standard line-impedance-stabilization-network (LISN). By noncontact paths we mean those paths that are not found in the original circuit diagram. They represent capacitive and inductive couplings of EMI noise from the circuit board to the LISN.

The paper is organized as follows. In Section II, we present the derivation of the model based on a circuit theoretic viewpoint. An illustration of the use of the model is given in Section III. In Section IV, we describe how the model can be applied in practical situations. Finally, an illustration of the procedure for estimating the parameters for the model is given in the Appendix, along with an experimental verification of the viability of lumped circuit representation for EMI prediction.

II. Lumped Circuit Model for Non-Contact EMI Based on Essential Coupling Paths

Our aim in this section is to derive a lumped circuit model for describing the essential coupling paths between the converter's circuit board and the LISN's physical input terminals. We assume a linear model for this application, and therefore the overall noise is equal to the sum of all components from individual analyzes for all harmonics. In the following we show the analysis for one particular harmonic.

A. Overview of Non-Contact Couplings

Fig. 1 shows the coupling of noise through noncontact paths from noise voltage sources on the circuit board to the LISN's input terminals L1, L2, and G. In Fig. (1a), we show the noise coupled capacitively from voltage sources on the circuit board and manifested as noise currents flowing into terminals L1, L2, and G. Let these noncontact noise currents that flow into the LISN be $I_{\mathrm{C,L1}}$, $I_{\mathrm{C,L2}}$, and $I_{\mathrm{C,G}}$, where subscript C denotes capacitive coupling.

Manuscript received April 9, 2002; revised October 21, 2002. This work was supported by the Hong Kong Special Administrative Region Government under the Innovation and Technology Fund (ITS/055/01). Recommended by Associate Editor K. Ngo.

N. K. Poon, B. M. H. Pong, and C. P. Liu are with the Department of Electrical and Electronic Engineering, University of Hong Kong, Pokfulam, Hong Kong, China (e-mail: nkpoon@eee.hku.hk; mhp@eee.hku.hk; cpliu@eee.hku.hk).

C. K. Tse is with the Department of Electronic and Information Engineering, Hong Kong Polytechnic University, Kowloon, Hong Kong, China (e-mail: encktse@polyu.edu.hk).

Digital Object Identifier 10.1109/TPEL.2003.809359

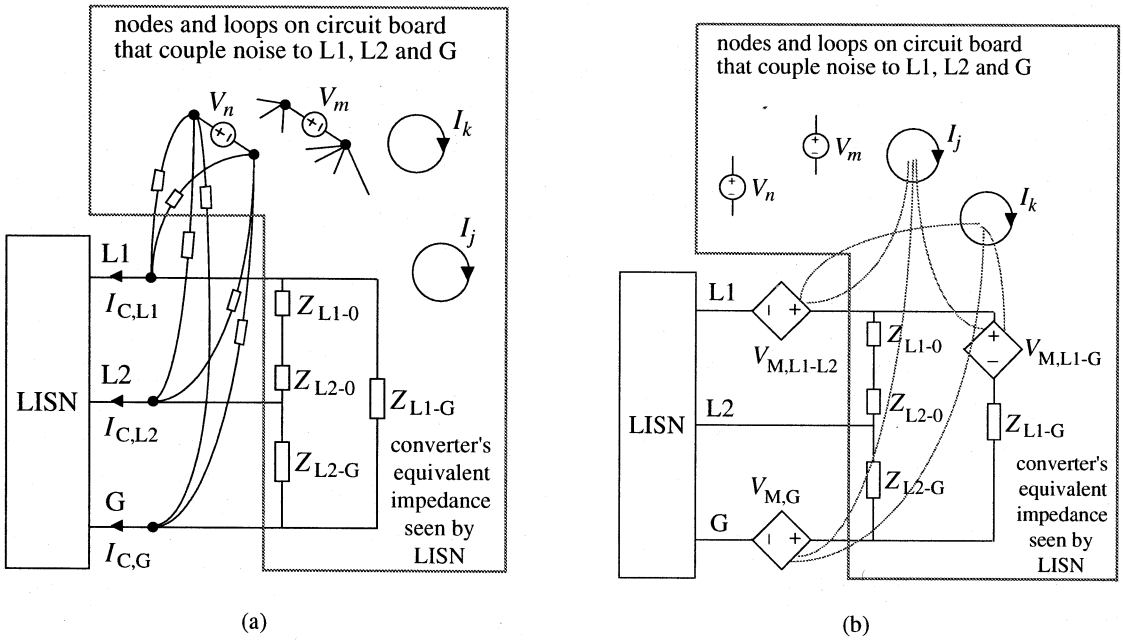

Fig. 1. (a) Noise coupled capacitively from noise voltage sources on the circuit board and manifested as noise currents flowing into terminals L1, L2 and G and (b) noise coupled inductively from current loops on the circuit board and manifested as controlled voltages applied around the loops formed by terminals L1, L2, and G and converter's equivalent impedances.

In a dual manner, Fig. 1(b) shows the inductive coupling of noise through noncontact paths from current loops on the circuit board to the LISN's input terminals L1, L2, and G. In this case, the appropriate induced noise sources are controlled voltage sources around the three loops formed between the LISN terminals and the converter's equivalent impedances. Note that the choice of the exact location in each loop is arbitrary. In Fig. 1(b), we denote the induced controlled voltages by $V_{\mathrm{M,L1-L2}}$, $V_{\mathrm{M,L1-G}}$, and $V_{\mathrm{M,G}}$, where subscript M denotes inductive coupling.

B. Derivation of the Lumped Circuit Model

The main modeling objective is to represent all coupling paths by a minimal number of noise sources and essential coupling paths. We begin with the capacitive coupling paths. Obviously, the simplest model consists of one equivalent noise voltage source which is connected to each terminal of the LISN through a coupling impedance. This requires a total of six impedances, as shown in Fig. 2(a). These six impedances constitute six *essential coupling paths* between the noise sources and the LISN terminals. Furthermore, since the noise sources are physically contained within the converter circuit, it is imperative that the noise voltage source is referenced to a node in the converter circuit. This node can be located arbitrarily, and a convenient choice is between L1 and L2, which is also regarded as the "zero reference" of the circuit. The equivalent model for capacitive coupling can then be represented by lumped circuit elements as shown in Fig. 2(a), where V_{eq} is the equivalent noise voltage source.

To complete the model, we need to include the inductively coupled noise. The same basic model shown in Fig. 1(b) can be used here, and the main modeling step is to replace all noise loop currents by one equivalent current source I_{eq}. A convenient choice is shown in Fig.2 (b), which depicts the complete lumped circuit model for all noncontact EMI coupled to the LISN.

In summary, the noncontact EMI in a switching converter can be represented by a lumped circuit model consisting of

1) an equivalent noise voltage, V_{eq}, which injects noise current to the LISN terminals via six coupling impedances (i.e., $Z_{\mathrm{C,L1,eq}}$, $Z_{\mathrm{C,L2,eq}}$, $Z_{\mathrm{C,G,eq}}$, $Z_{\mathrm{C,L1,0}}$, $Z_{\mathrm{C,L2,0}}$, and $Z_{\mathrm{C,G,0}}$);
2) an equivalent noise current, I_{eq}, which induces noise voltage to the three loops formed around the converter's impedances and the LISN terminals, the coupling impedances being $Z_{\mathrm{M,L1-L2}}$, $Z_{\mathrm{M,L1-G}}$, and $Z_{\mathrm{M,G}}$.

Based on the above model, the noise currents coupled capacitively from the converter circuit to the LISN terminals and the noise voltages coupled inductively from the converter circuit to the terminal loops can be written in terms of the equivalent noise voltage and current sources and the coupling impedances. Assuming that V_{L1}, V_{L2}, and V_{G} are the voltages at L1, L2, and G with respect to the zero reference, and setting $Z_{C,0}$ to 0, we have

$$I_{\mathrm{C,L1}} = \frac{V_{\mathrm{eq}} - V_{\mathrm{L1}}}{Z_{\mathrm{C,L1,eq}}} - \frac{V_{\mathrm{L1}}}{Z_{\mathrm{C,L1,0}}} \tag{1}$$

$$I_{\mathrm{C,L2}} = \frac{V_{\mathrm{eq}} - V_{\mathrm{L2}}}{Z_{\mathrm{C,L2,eq}}} - \frac{V_{\mathrm{L2}}}{Z_{\mathrm{C,L2,0}}} \tag{2}$$

$$I_{\mathrm{C,G}} = \frac{V_{\mathrm{eq}} - V_{\mathrm{G}}}{Z_{\mathrm{C,G,eq}}} - \frac{V_{\mathrm{G}}}{Z_{\mathrm{C,G,0}}} \tag{3}$$

$$V_{\mathrm{M,L1-L2}} = I_{\mathrm{eq}} Z_{\mathrm{M,L1-L2}} \tag{4}$$

$$V_{\mathrm{M,L1-G}} = I_{\mathrm{eq}} Z_{\mathrm{M,L1-G}} \tag{5}$$

$$V_{\mathrm{M,G}} = I_{\mathrm{eq}} Z_{\mathrm{M,G}}. \tag{6}$$

It should be reiterated that the above model does not include direct-contact EMI, such as input ripple current, which can be

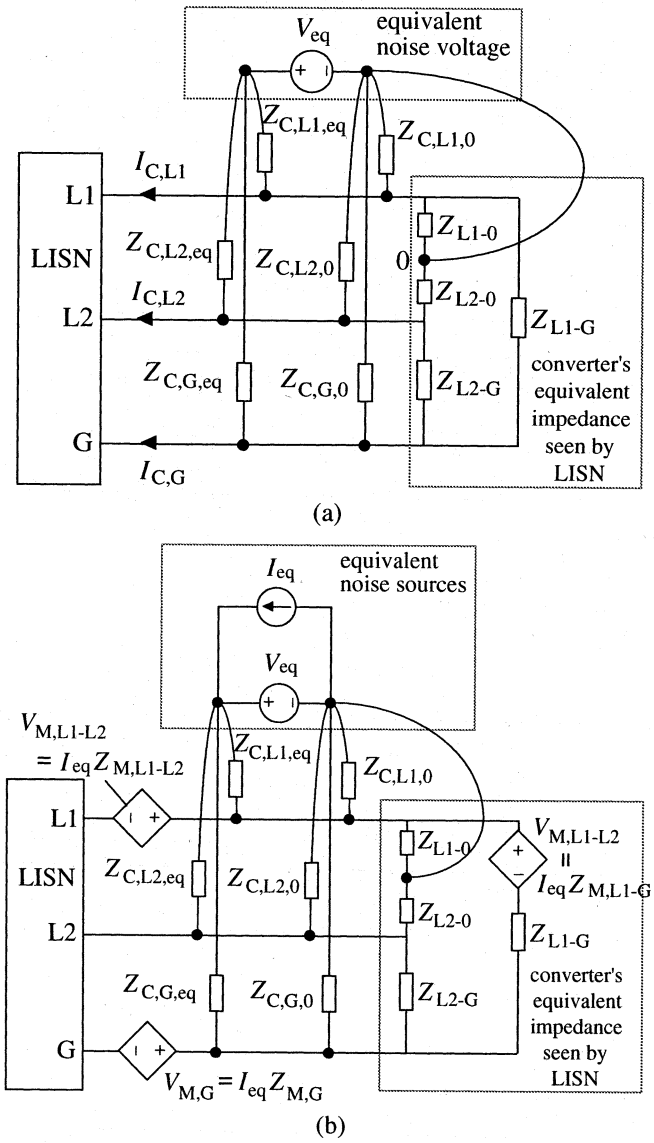

Fig. 2. (a) Lumped circuit model for noncontact paths via capacitive coupling and (b) complete lumped circuit model for noncontact paths.

modeled by current source(s) that are directly connected to the LISN terminals.

Here we emphasize that the equivalent noise sources are necessary and sufficient, and all coupling paths in the model are essential. The resulting model therefore provides a guiding model for evaluating the effects of all noncontact couplings. Moreover, the model still requires parameter estimation in order to be practically useful. The estimation of parameters for the model can be done by measurement or analytical calculation based on the geometry of the circuit. Furthermore, using this guiding model, engineers may identify significant coupling paths more easily on the one hand, and may less easily ignore some subtle but important coupling paths on the other hand.

C. Physical Interpretation

The afore-derived lumped circuit model can be easily applied to practical situations. Consider a boost converter, for example. Suppose the capacitively coupled noise is dominated by the switching noise across the transistor's drain and source. Then, we may approximate the equivalent voltage source $V_{\rm eq}$ as the voltage across the drain and source of the transistor, assuming that all other physical noise sources are negligible. Let the capacitance between the transistor's drain node and ground be $C_{\rm C,G-eq}$. The situation is shown in Fig. 3. Thus, the coupling impedance $Z_{\rm C,G-eq}$ can be approximated by

$$Z_{\rm C,G-eq} = \frac{1}{sC_{\rm C,G-eq}} \tag{7}$$

which is simply the total switching-node-to-ground capacitance. The other coupling impedances can also be approximated in a likewise manner, as illustrated in Fig. 3(b). Specifically, we have

$$Z_{\rm C,L1-eq} = \frac{1}{sC_{\rm C,L1-eq}} \tag{8}$$

$$Z_{\rm C,L2-eq} = \frac{1}{sC_{\rm C,L2-eq}} \tag{9}$$

where $C_{\rm C,L1-eq}$ and $C_{\rm C,L2-eq}$ are the total switching-node-to-line capacitances. In practice, the switching node is often identified as "hot" node in the analysis of EMI problems. The hot-node-to-ground capacitance, $C_{\rm C,G-eq}$, has been studied by many authors [8]–[10], [19]–[21]. However, the other two capacitances, namely hot-node-to-line capacitances, are rarely discussed [9], [11].

Furthermore, there are three coupling impedances associated with the zero reference node, i.e., $Z_{\rm C,L1,0}$, $Z_{\rm C,L2,0}$ and $Z_{\rm C,G,0}$. They can be approximated by the corresponding capacitances between each of the LISN terminals to the circuit's zero reference node, i.e.,

$$Z_{\rm C,L1-0} = \frac{1}{sC_{\rm C,L1-0}} \tag{10}$$

$$Z_{\rm C,L2-0} = \frac{1}{sC_{\rm C,L2-0}} \tag{11}$$

$$Z_{\rm C,G-0} = \frac{1}{sC_{\rm C,G-0}} \tag{12}$$

where $C_{\rm C,L1-0}$ and $C_{\rm C,L2-0}$ are the total "zero"-to-line capacitances, which represent rather subtle coupling paths, and $C_{\rm C,G-0}$ is the total "zero"-to-ground capacitance and can be approximated as the converter-to-ground capacitance. Usually, $C_{\rm C,G-0}$ has a much higher value compared to the other capacitances, and therefore undesirably produces a low-impedance loop which permits significant noise current to circulate due to the inductively coupled noise voltage $V_{\rm M,G}$. See Fig. 3(c). This effect of low-impedance loop caused by large $C_{\rm C,G-0}$ is rarely discussed [21].

III. Illustrative Example—Parameter Estimation and EMI Prediction

In this section, we illustrate the estimation of the parameters in the afore-described model, and demonstrate the significance of each coupling path in producing conducted EMI. We will use these estimated parameters again in Section IV for predicting EMI in a practical boost converter.

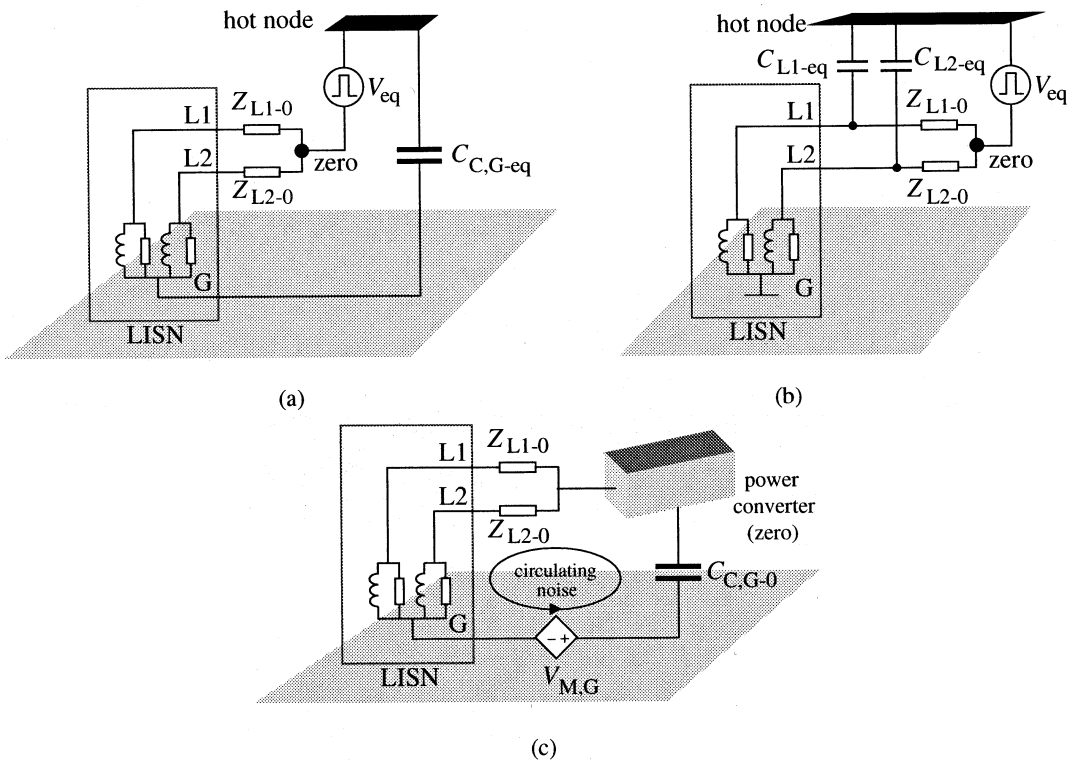

Fig. 3. Physical interpretation of the coupling impedances and paths.

A. Model Parameters for Capacitive Coupling

To use the model, we need to supply the actual values of the parameters including the noise sources and the coupling impedances. First, we define $V_{\rm eq}$ as a voltage pulse with the following parameters:

peak value	:	400 V
duty cycle	:	0.3
rise time	:	150 ns
fall time	:	20 ns
frequency	:	150 kHz.

We now consider the coupling impedances. As explained earlier, we have more impedances than are needed to define $I_{\rm C,L1}$, $I_{\rm C,L2}$ and $L_{\rm C,G}$ independently. However, to preserve the physical meanings, we include six essential coupling impedances in the model, namely, $Z_{\rm C,L1,eq}$, $Z_{\rm C,L2,eq}$, $Z_{\rm C,G,eq}$, $Z_{\rm C,L1,0}$, $Z_{\rm C,L2,0}$ and $Z_{\rm C,G,0}$. To simplify the model, we may assume that $V_{\rm eq}$ is connected to the zero reference of the converter and hence $Z_{\rm C,0}=0$.

We assume that the "hot" node is a thin copper trace of width $W=0.1$ cm, length $l=4$ cm, thickness $t=0.01$ cm, and distance to ground $R=40$ cm. The capacitance to ground can be approximated based on a sphere with surface area Wl [2], i.e.,

$$C_{\rm sphere}=\frac{4\pi(0.085)}{\frac{1}{r}}{\rm pF} \tag{13}$$

which is one of the coupling impedances in our model, i.e.,

$$Z_{\rm C,G,eq}=\frac{1}{sC_{\rm C,G,eq}} \text{ with } C_{\rm C,G,eq}=0.2\ {\rm pF}. \tag{14}$$

Suppose in the printed circuit board the "hot" trace is running in parallel with traces of L1 and L2. The distance between the "hot" trace and the L1 trace is 5 cm, and that between the "hot" trace and the L2 trace is 5.4 cm. Further assume that the width, length and thickness of these traces are 0.1 cm, 2 cm and 0.01 cm, respectively. Thus, the trace-to-trace capacitance can be approximated as

$$C_{\rm trace-trace}=\frac{14(\epsilon_r+1)}{\ln\frac{\pi s}{W+t}}{\rm pF/m} \tag{15}$$

which can be used to find $Z_{\rm C,L1,eq}$ and $Z_{\rm C,L2,eq}$ of the model. Putting in the appropriate values gives

$$C_{\rm C,L1,eq}=0.005\,604\ {\rm pF} \quad \text{and} \quad C_{\rm C,L2,eq}=0.005\,518\ {\rm pF}. \tag{16}$$

Hence, $Z_{\rm C,L1,eq}=1/sC_{\rm C,L1,eq}$ and $Z_{\rm C,L2,eq}=1/sC_{\rm C,L2,eq}$.

To estimate $Z_{\rm C,G,0}$, we assume that the power converter is a spherical body [2] and the converter-to-ground capacitance is its self capacitance, i.e.,

$$Z_{\rm C,G,0}=\frac{1}{sC_{\rm C,G,0}} \text{ with } C_{\rm C,G,0}\approx C_{\rm self}=\frac{4\pi(0.085)}{\frac{1}{r}} =6\,{\rm pF}. \tag{17}$$

The remaining two coupling impedances to be found are $Z_{\rm C,L1,0}$ and $Z_{\rm C,L2,0}$. Clearly, these impedances can be absorbed into $Z_{\rm L1-0}$ and $Z_{\rm L2-0}$, as shown in Fig. (2b). Now, by measurement (using HP4194 impedance analyzer), we find that $Z_{\rm L1-0}$ and $Z_{\rm L2-0}$ are mainly inductive and given by

$$Z_{\rm C,L1,0}=(108\ \mu{\rm H}+16\ \Omega)||(27\ {\rm pF}) \tag{18}$$

$$Z_{\rm C,L2,0}=(51\ \mu{\rm H}+6\ \Omega)||(14\ {\rm pF}). \tag{19}$$

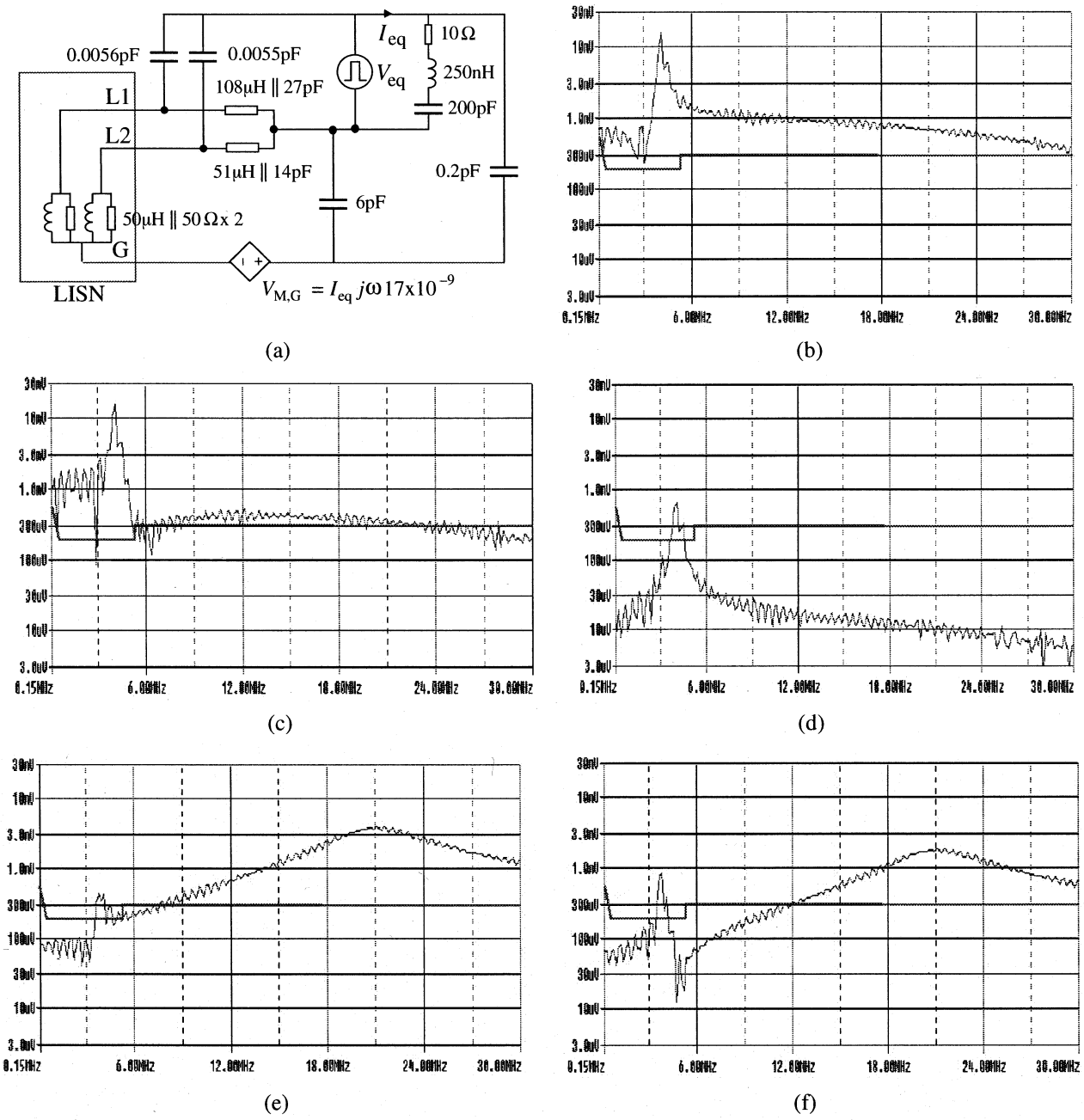

Fig. 4. Simulation with parameter values estimated or measured, showing the significance of each coupling path. (a) Circuit model; (b) noise picked up by LISN L1 with $C_{\mathrm{C,G-eq}}$ only; (c) noise picked up by LISN L2 with $C_{\mathrm{C,G-eq}}$ only; (d) noise picked up by LISN L1 or L2 with $C_{\mathrm{C,L1-eq}}$ and $C_{\mathrm{C,L2-eq}}$ only; (e) noise picked up by LISN L1 with $C_{\mathrm{C,G-0}}$ only; (f) noise picked up by LISN L1 with $C_{\mathrm{C,G-0}}$ only. Limit lines shown in (b) to (f) are based on EN55022 average noise limits.

B. Model Parameters for Inductive Coupling

We now consider the inductive coupling. As shown in Fig. 2(b), inductive couplings are modeled by three controlled voltage sources applied around three loops formed between L1, L2, G and the converter. Induced by I_{eq}, the effect of these controlled voltage sources depends very much on the overall impedance around the loop concerned. It has also been mentioned previously that among the three controlled voltage sources, $V_{\mathrm{M,G}}$ is usually quite significant because of the low impedance loop. In the following, we only attempt to find $Z_{\mathrm{M,G}}$. Nonetheless, we should stress that the other two coupling impedances may also be important in some situations, but they are not easily identified in practice.

First, a reasonable assumption for I_{eq} is that it actually emulates the current which flows in a series LCR element connected across V_{eq}. Physically this LCR element represents parasitics along a loop through the switching converter, which typically includes the parasitic capacitance in the windings of the main power transformer, snubber circuits, connection inductances and resistances. The following is a realistic set of values for this LCR element:

$$L = 250 \text{ nH}, \; C = 200 \text{ pF} \quad \text{and} \quad R = 10\ \Omega.$$

Suppose the loop formed by $I_{\rm eq}$ and the LCR element is an equivalent circle of radius 2 cm. We focus on the coupling of this circle loop to the loop containing the line cable (composed of L1 and L2) and ground. Since the cable length (typically 1 meter long) is much larger than the loop radius, we may apply the standard formula for the mutual inductance between a circle loop and a long straight wire [20]

$$L_{\rm loop-to-line} = \mu_0 \left[\frac{L}{2} - \sqrt{\left(\frac{L}{100}\right)^2 - \left(\frac{r}{100}\right)^2} \right] \text{H} \quad (20)$$

where L is the distance of the circle loop to the wire and r is the radius of the circle loop. Assuming that the loop radius r is 1.9 cm and the distance L is 2 cm, we have

$$Z_{\rm M,G} = sL_{\rm M,G} \quad \text{with} \quad L_{\rm M,G} = 17 \text{ nH}. \quad (21)$$

Hence, we have all the parameters for the complete lumped circuit model, as shown in Fig. 4(a).

C. Significance of the Coupling Paths

In this subsection we present simulation results to demonstrate the significance of each coupling path. Fig. 4(a) shows the model used for simulation. Fig. 4(b) and 4(c) show the simulated noise spectra picked up by the LISN (L1 and L2) when $C_{\rm C,G,eq}$ (0.2 pF) is present alone. These figures represent the so-called *common mode* noise, which is due to the coupling path through $C_{\rm C,G,eq}$. The resonant peak near 4 MHz is caused by the input impedances $Z_{\rm L1-0}(108\ \mu\text{H}||27\text{ pF})$ and $Z_{\rm L1-0}(51\ \mu\text{H}||14\text{ pF})$.

Fig. 4(d) shows the simulated noise spectrum picked up by the LISN (L1 or L2) due to the presence of $C_{\rm C,L1,eq}$(0.0056 pF) and $C_{\rm C,L2,eq}$(0.0055 pF) which is connect the input lines to the "hot" node. Here, we observe a resonant peak near 4 MHz, which is again due to $Z_{\rm L1-0}$ and $Z_{\rm L1-0}$.

Figs. (4e) and (f) show the simulated noise spectra picked up by the LISN (L1 and L2) due to the induced voltage source $V_{\rm M,G}$. This voltage is applied to the loop containing $C_{\rm C,G,0}$(6 pF). Here, two resonant peaks are observed. The first one near 4 MHz is caused by $Z_{\rm L1-0}$, $Z_{\rm L1-0}$ and $C_{\rm M,G}$, and the second one near 22 MHz is caused by the LCR element connected in parallel with $V_{\rm eq}$.

Clearly, our simulations show that each coupling path can produce significant noise at the LISN, especially at frequencies near the resonant peaks. This is consistent with what is often observed in practice, where the noise spectrum captured by the LISN often exhibits resonant peaks.

IV. Application and Experimental Verification

In this section we describe an application of the proposed lumped circuit modeling approach for predicting noncontact EMI in a practical boost converter. The parameters associated with the lumped circuit model are those found earlier in Section III. We will perform simulations of the EMI and confirm the prediction by experimental measurements.

Fig. 5(a) shows the prototype boost converter under test, and Fig. 5(b) shows the PSPICE schematic for the proposed lumped circuit model, which includes all coupling paths. The input filter, formed by C_1, C_2 and $L_{\rm L3}$, reduces the input ripple to an negligible amount. Also, C_4 emulates the presence of a snubber.

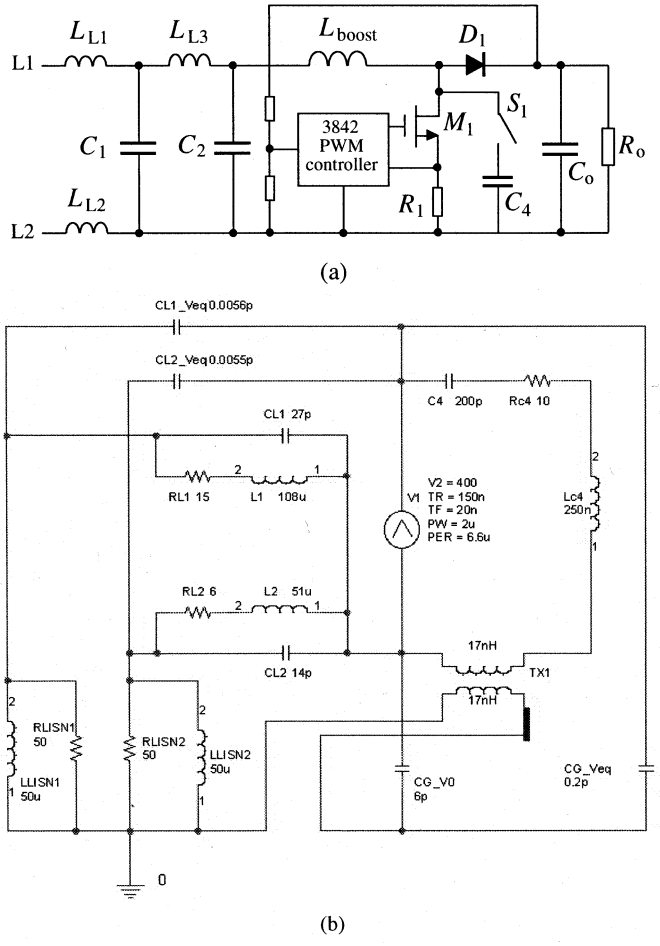

Fig. 5. (a) Simplified schematic of the boost converter and (b) PSPICE circuit showing details of parasitic impedances (e.g., $L_{\rm L1}$ and $L_{\rm L2}$) and the lumped circuit model of essential coupling paths.

When the mechanical switch S_1 is closed, a loop is formed containing the "hot" noise voltage, C_4 and some parasitic inductance and resistance. This loop actually corresponds to the $I_{\rm eq}$ in the lumped circuit model developed earlier in Section 2. We can therefore isolate capacitive coupling from inductive coupling by opening or closing S_1. Specifically, with S_1 opened, we only look at capacitive coupling, and with S_1 closed, we look at both capacitive and inductive couplings. The converter circuit parameters used are

$L_{\rm boost}$	:	2 mH
$L_{\rm L3}$ (input filter)	:	500 μH
C_1, C_2 (input filter)	:	330 μF
C_4 (representing snubber loop)	:	200 pF
duty cycle	:	0.3
output power	:	20 W
switching frequency	:	150 kHz
output voltage	:	400 V.

We first consider the case with S_1 opened. This corresponds to the situation where the snubber capacitance is absent, thus eliminating inductive coupling. In the simulation, we simply set C_4 to zero. Experimental results are shown in Fig. 6(a) and 6(b),

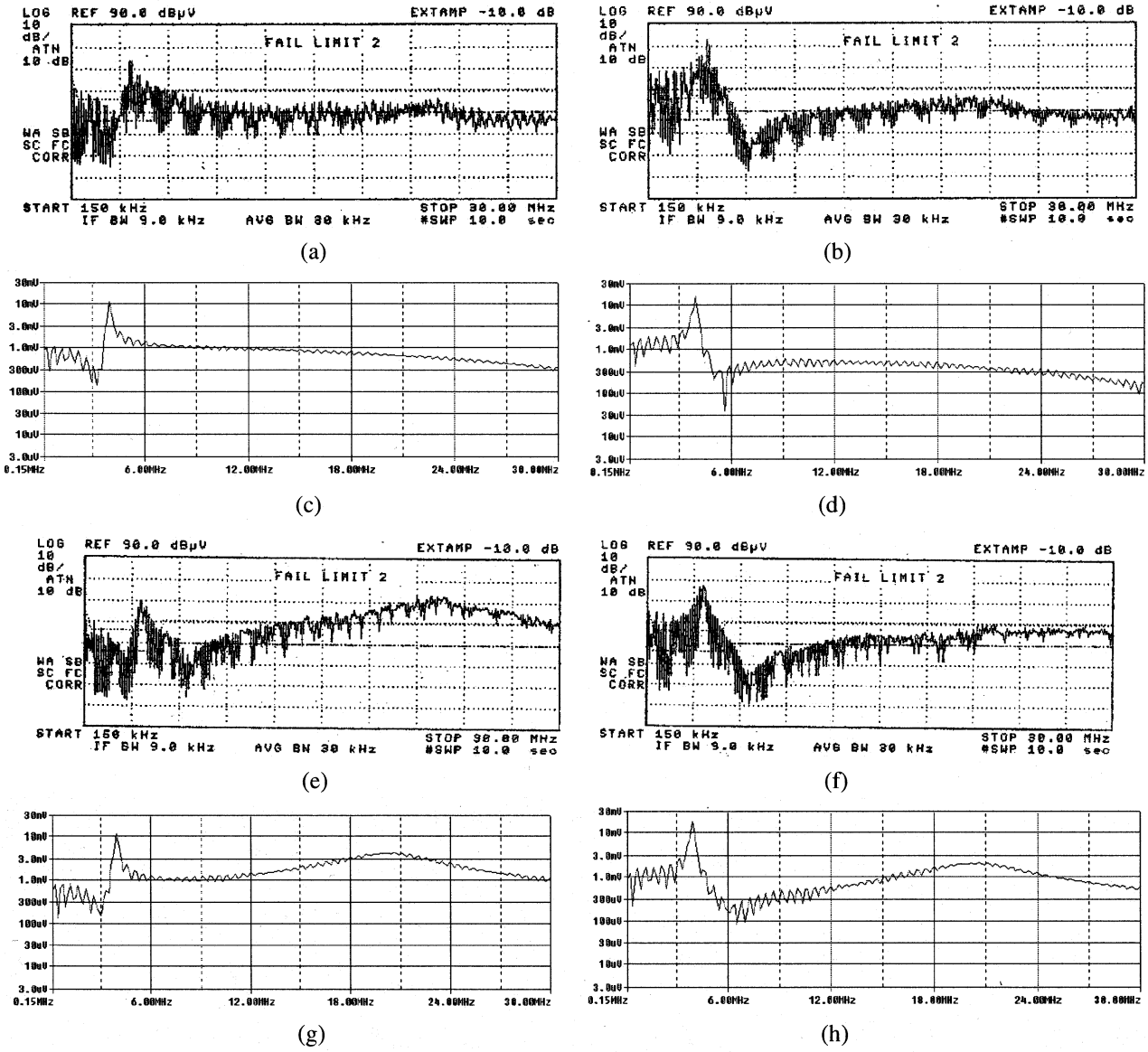

Fig. 6. Measured and simulated noise current spectra for the boost converter prototype: (a) measured noise spectrum at LISN L1 with S_1 opened (capacitive coupling only); (b) measured noise spectrum at LISN L2 with S_1 opened (capacitive coupling only); (c) simulated noise spectrum at LISN L1 with S_1 opened (capacitive coupling only); (d) simulated noise spectrum at LISN L2 with S_1 opened (capacitive coupling only); (e) measured noise spectrum at LISN L1 with S_1 closed (capacitive and inductive couplings); (f) measured noise spectrum at LISN L2 with S_1 closed (capacitive and inductive couplings); (g) simulated noise spectrum at LISN L1 with S_1 closed (capacitive and inductive couplings); and (h) simulated noise spectrum at LISN L2 with S_1 closed (capacitive and inductive couplings).

whereas simulated results are shown in Fig. 6(c) and 6(d). As shown consistently in both sets of results, there is a resonant peaking near 4 MHz. This has been explained in Section III as being resulted from the input impedances $L_{\rm L1}$ and $L_{\rm L2}$. Here, we confirm that the model indeed predicts this resonant peaking quite accurately.

Next, we close S_1, thus making inductive coupling a major player. Experimental results are shown in Fig.6 (e) and 6(f), whereas simulated results are shown in Fig. 6(g) and 6(h). Again, both sets of results indicate an extra resonant peaking at around 20 MHz, in addition to the one near 4 MHz. This high-frequency peaking, as explained earlier in Section III, is caused by the inductive coupling loop (excitation loop) which is formed by C_4 and some parasitic inductance and resistance.

From this application example, we see that the lumped circuit model indeed provides an adequate means for studying noncontact EMI up to around 30 MHz. However, it should be noted that we have not yet addressed the effects of $V_{\rm M,L1-L2}$ and $V_{\rm M,L1-G}$ which also form part of the inductive coupling model. The difficulty in analyzing these sources lies mainly in the identification of the corresponding mutual inductances. Nonetheless, it should be borne in mind that they may make a significant contribution to the EMI behavior in some situations.

V. Conclusion

EMI prediction is never an easy task. Subtle coupling paths often present a major source of confusion in the analysis of EMI

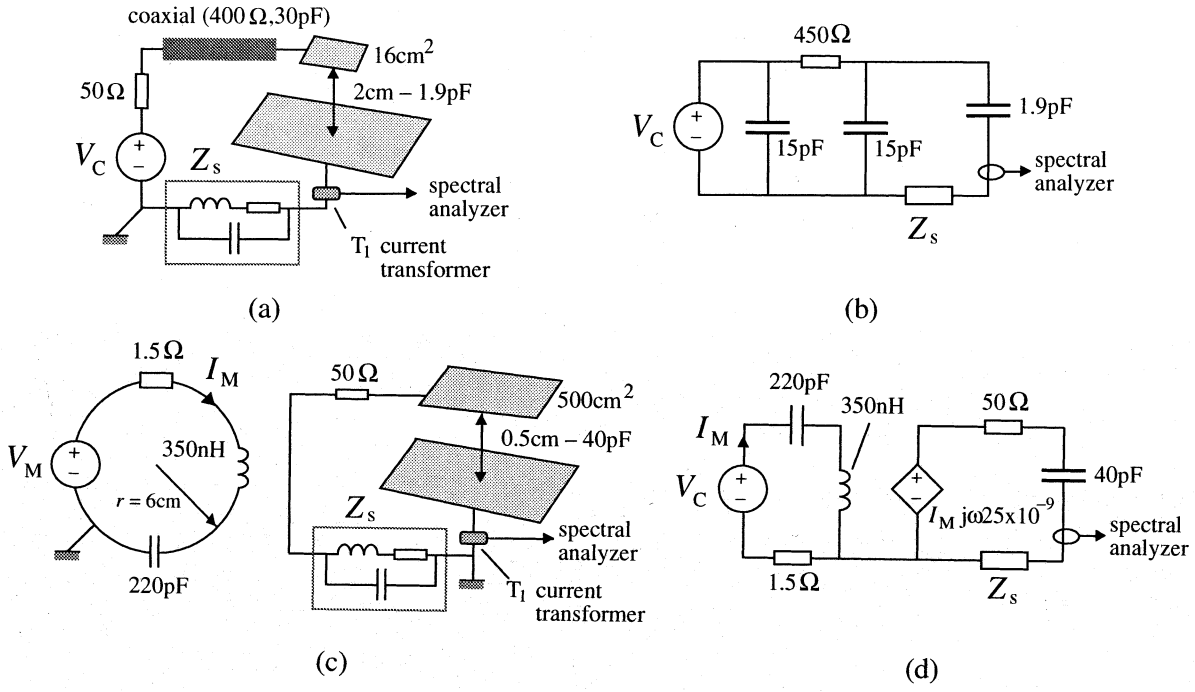

Fig. 7. (a) Physical construction and (b) equivalent circuit of the experimental setup for verifying the lumped circuit model for *capacitively coupled* noise; (c) physical construction and (d) equivalent circuit of the experimental setup for verifying the lumped circuit model for *inductively coupled* noise.

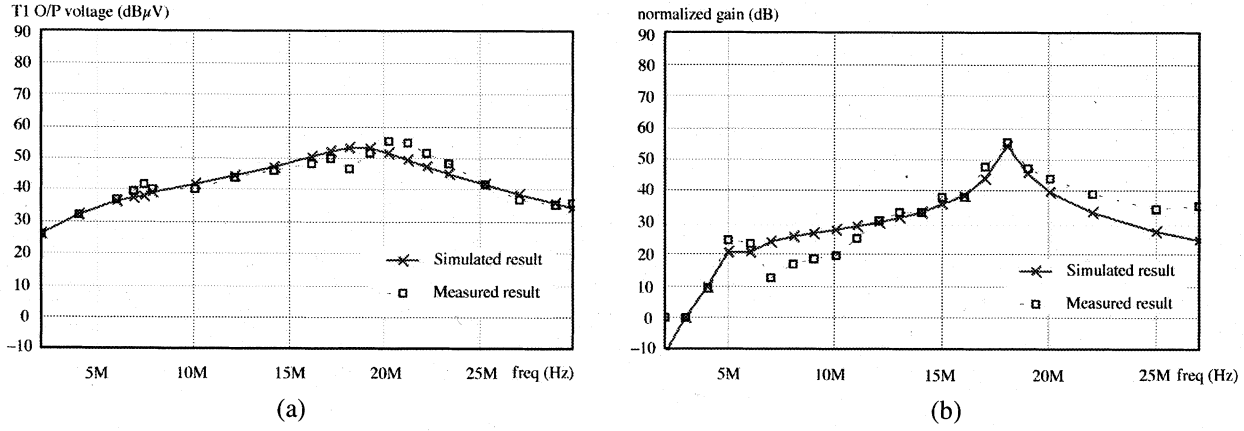

Fig. 8. Verification of the lumped circuit model. Simulated and measured noise current spectra for (a) capacitive coupling and (b) inductive coupling.

problems. In this paper we attempt to provide a systematic approach for modeling all noncontact EMI, which can be summarized as follows.

1) We analyze the basic problem from the viewpoint of capacitive and inductive couplings and make an attempt to represent the noncontact EMI in terms of one voltage source and one current source which couple noise to the LISN terminals via coupling impedances.
2) We systematically identify six capacitive coupling paths which directly inject noise currents into the LISN terminals.
3) For inductive coupling, our model simply includes three controlled voltage sources applied around the three loops formed between the LISN terminals and the converter's equivalent impedances. The circulating currents therefore flow into the LISN, especially for the low-impedance loop(s).
4) The model parameters are the noise sources and the essential coupling impedances. The problem thus reduces to finding the (dominant) noise sources and all relevant coupling impedances either by calculation or by measurement.

Since the model is based on lumped circuits, its validity is limited to frequencies below around 30 MHz. Moreover, in using the model for predicting EMI, one should bear in mind that no exact prediction can be expected from the model. First of all, the actual couplings are far more complicated than what a simple lumped circuit can possibly predict. The proposed model provides a simple (yet adequate) means to make an initial estimation of the extent of the interference. Second, the

parameter values can never be estimated accurately. However, it usually suffices to make some simplifying assumptions on the geometry of the circuit tracks and components in order to get a quick estimate of the coupling impedances. In conclusion we should stress that complicated problems such as EMI may require tedious and complex analysis if highly accurate solutions are to be sought. However, in practical engineering, there is always a need to trade off accuracy for simplicity. In this case we have demonstrated a simple yet viable approach to the EMI problem based on a simple lumped circuit model. This model contains the salient features of noncontact EMI, is convenient to use, and gives adequate prediction of EMI behavior in switching converters.

APPENDIX

VERIFICATION OF THE VIABILITY OF THE LUMPED CIRCUIT MODEL

In this appendix we present two separate experiments to verify the adequacy of lumped circuit models for predicting the capacitively coupled and the inductively coupled EMI.

The experimental setup for verifying the lumped circuit model for capacitively coupled EMI is shown in Fig. 7(a). The model basically consists of a small piece of metal plate hanging above a large plate emulating the capacitive coupling between a node and ground. Also, a voltage generating $V_{\rm C} = 1$ V (peak), with an output resistance of 50 Ω, is applied across the two plates through a coaxial cable and a series impedance, Z_s, consisting of inductance, capacitance and resistance. The capacitance between the plates is found to be 1.9 pF (using a finite element software). This capacitance is analogous to the hot-node-to-ground capacitance in our model. The equivalent circuit is shown in Fig. 7(b). Here, the 450 Ω resistor represents the combined resistance of the voltage source's (50 Ω) and the coaxial cable's (400 Ω). Together with the two 15 pF capacitors they form a simple distributed model for the coaxial cable.

The setup for verifying the lumped circuit model for inductively coupled EMI is shown in Fig. 7(c). A large metal plate representing the converter is hung above a much larger plate that represents the ground. The capacitance between the plates is therefore analogous to the converter-to-ground capacitance in our model. By measurement (using HP4194 impedance analyzer), this capacitance is found to be 40 pF. The two plates are then connected by a resistor of 50 Ω and an impedance Z_s, forming a closed loop through which induced noise can circulate. Now we need another loop to emulate the noise excitation. This excitation loop is constructed as shown on the left of Fig. 7(c), and is located at a distance 10 cm from the first loop. The excitation voltage $V_{\rm M}$ is 0.5 V (peak), and the frequency runs from 150 kHz to 30 MHz. Inductive coupling thus occurs between the two loops. The mutual inductance can be estimated using (20), and is approximately 25 nH. The equivalent circuit is shown in Fig. 7(d).

The current transformer T_1 in both setups is used to pick up the noise current. It has a conversion ratio of 1 μA to 0.5 μV when terminated to a 50 Ω load. The noise current can then be read out from a spectral analyzer as shown in Fig. 7(a) and 7(c).

Finally, the impedance Z_s, which has been included to emulate the parasitic impedance, is constructed by a wire wound inductor on a ferrite core. Its equivalent circuit is shown in Fig. 7(a) and 7(c). The measured values of the constituent inductance, resistance and capacitance are 13 μH, 7 Ω and 5 pF for frequencies below 5 MHz, and are 11.4 μH, 333 Ω and 1.5 pF for frequencies between 5 MHz and 30 MHz.

Fig. 8(a) and 8(b) show the simulated and measured results for the capacitive coupling and inductive coupling cases for frequencies below 30 MHz, i.e., the conducted EMI range. It is clear that simulation results using the lumped circuit model is in good agreement with the measurements.

REFERENCES

[1] J. P. Mill, *Electromagnetic Interference Reduction in Electronic Systems*. Englewood Cliffs, NJ: Prentice Hall, 1993.

[2] T.Tim Williams, *EMC for Product Designers*. London, U.K.: Butterworth-Heinemann Ltd., 1994.

[3] M. D. Herema, *Designing for Electromagnetic Compatibility*. New York: Hewlett Packard, 1995.

[4] M. K. W. Wu and C. K. Tse, "A review of EMI problems in switch mode power supply design," *J. Elect. Electron. Eng. Australia*, vol. 16, no. 3&4, pp. 193–204, 1996.

[5] E. Laboure, F. Costa, C. Gautier, and W. Melhem, "Accurate simulation of conducted interferences in isolated dc to dc converters regarding to EMI standards," in *Proc. IEEE Power Electron. Spec. Conf.*, 1996, pp. 1973–1978.

[6] W. Zhang, M. T. Zhang, F. C. Lee, J. Roudet, and E. Clavel, "Conducted EMI analysis of a boost PFC circuit," in *Proc. IEEE Applied Power Electron. Conf. Exp.*, 1997, pp. 223–229.

[7] J. A. Ferreira, P. R. Willcock, and S. R. Holm, "Sources, paths and traps of conducted EMI in switch mode circuits," in *Proc. IEEE Ind. Applicat. Conf.*, 1997, pp. 1584–1591.

[8] Q. Chen, "Electromagnetic interference (EMI) design considerations for a high power ac/dc converter," in *Proc. IEEE Power Electron. Spec. Conf.*, 1997, pp. 1159–1164.

[9] B. M. H. Pong and A. C. M. Lee, "A method to measure EMI due to electric field coupling on PCB," in *Proc. Power Conv. Conf.*, 1997, pp. 1007–1012.

[10] D. Zhang, D. Chen, and D. Sable, "Non-intrinsic differential mode noise caused by ground current in an off-line power supply," in *Proc. IEEE Power Electron. Spec. Conf.*, 1998, pp. 1131–1133.

[11] M. H. Pong, C. M. Lee, and X. Wu, "EMI due to electric field coupling on PCB," in *Proc. IEEE Power Electron. Spec. Conf.*, 1998, pp. 1125–1130.

[12] M. K. W. Wu, C. K. Tse, and P. Chan, "Development of an integrated CAD tool for switching power supply design with EMC performance evaluation," *IEEE Trans. Ind. Applicat.*, vol. 34, pp. 364–373, Mar./Apr. 1998.

[13] M. Joshi and V. Agarwal, "Generation and propagation of EMI waves in power electronic circuits," in *Proc. IEEE Power Electron. Spec. Conf.*, 1998, pp. 1165–1171.

[14] P. F. Okyere and L. Heinemann, "Computer-aided analysis and reduction of conducted EMI in switched-mode power converter," in *Proc. IEEE Appl. Power Electron. Conf. Exp.*, 1998, pp. 924–928.

[15] D. F. Knurek, "Reducing EMI in switch mode power supplies," in *Proc. Int. Telecom. Energy Conf.*, 1998, pp. 411–420.

[16] M. Cacciato, C. Cavallaro, G. Scarcella, and A. Testa, "Effects of connection cable length on conducted EMI in electric drives," in *Proc. Int. Conf. Elect. Mach. Drives*, 1999, pp. 428–430.

[17] L. Rossetto, S. Buso, and G. Spiazzi, "Conducted EMI issues in a 600-W single-phase boost PFC design," *IEEE Trans. Ind. Applicat.*, vol. 36, pp. 578–585, Mar./Apr. 2000.

[18] M. N. Gitau, "Modeling conducted EMI noise generation and propagation in boost converters," in *Proc. IEEE Int. Symp. Ind. Electron.*, 2000, pp. 353–358.

[19] T. Ninomiya, M. Shoyama, C. F. Jin, and G. Li, "EMI issues in switching power converters," in *Proc. Int. Symp. Power Semicond. Devices ICs*, 2001, pp. 81–86.

[20] D. K. Cheng, *Fields, Waves and Electromagnetics*, 2nd ed. Reading, MA: Addison-Wesley, 1989.

[21] N. K. Poon, C. P. Liu, and M. H. Pong, "Least coupling paths model for noncontact EMI based on lumped element approach in switch mode converter," in *Proc. IEEE Power Electron. Spec. Conf.*, 2001, pp. 577–582.

N. K. Poon (M'95) received the B.Eng. (with honors) degree in electronic engineering from the City University of Hong Kong, Kong Kong, in 1995 and is currently pursuing the Ph.D. degree at Hong Kong Polytechnic University.

After graduation he worked with Artesyn Technologies (Asia Pacific), Ltd., for three and a half years before joining the Power Electronics Laboratory, University of Hong Kong. His current interest includes soft switching techniques, EMI modeling, PFC topologies, synchronous rectification, converter modeling, PWM inverters, and fast transient regulators.

Bryan M. H. Pong (M'84–SM'96) was born in Hong Kong. He received the B.Sc. degree in electronic and electrical engineering from the University of Birmingham, Birmingham, U.K., in 1983 and the Ph.D. degree in power electronics from Cambridge University, Cambridge, U.K., in 1987.

After graduation, he became a Senior Design Engineer and then a Chief Design Engineer at National Semiconductor Hong Kong, where he was involved in electronic product design. Afterwards he joined ASTEC International, Hong Kong, first as a Principal Engineer and then a Division Engineering Manager. He is now an Associate Professor with the University of Hong Kong, Hong Kong, where he is in charge of the Power Electronics Laboratory and leads a team to carry out research in switching power supplies. His research interests include synchronous rectification, EMI issues, power factor correction, magnetic component design, and soft switching. He is co-holder of a number of U.S. patents.

C. P. Liu (M'99) was born in Hong Kong in 1970. He received the B.S. degree in electrical and electronic engineering from the University of Hong Kong, Hong Kong, in 1993.

From 1993 to 1999, he held several industrial positions in switching power supply design. Since 1999, he has been with the Power Electronics Laboratory, University of Hong Kong, where he is a Principal Engineer. His research interest includes switching converter topologies, synchronous rectifiers, soft switching, and EMI modeling.

Chi K. Tse (M'90–SM'97) received the B.Eng. degree (with first class honors) in electrical engineering and the Ph.D. degree from the University of Melbourne, Australia, in 1987 and 1991, respectively.

He is presently a Professor with Hong Kong Polytechnic University, Hong Kong, and his research interests include chaotic dynamics and power electronics. He is the author of *Linear Circuit Analysis* (London, U.K.: Addison-Wesley, 1998), co-author of *Chaos-Based Digital Communication Systems* (Heidelberg, Germany: Springer-Verlag, 2003), and co-holder of a U.S. patent. Since 2002, he has been appointed as Advisory Professor by the Southwest China Normal University, Chongqing, China.

Dr. Tse received the L.R. East Prize by the Institution of Engineers, Australia, in 1987, the IEEE Transactions on Power Electronics Prize Paper Award, in 2001, the President's Award for Achievement in Research, twice, and the Faculty's Best Researcher Award. He was an Associate Editor for the IEEE TRANSACTIONS ON CIRCUITS AND SYSTEMS PART I—FUNDAMENTAL THEORY AND APPLICATIONS, from 1999 to 2001, and since 1999 he has been an Associate Editor for the IEEE TRANSACTIONS ON POWER ELECTRONICS.